



This open access document is published as a preprint in the Beilstein Archives with doi: 10.3762/bxiv.2019.95.v1 and is considered to be an early communication for feedback before peer review. Before citing this document, please check if a final, peer-reviewed version has been published in the Beilstein Journal of Organic Chemistry.

This document is not formatted, has not undergone copyediting or typesetting, and may contain errors, unsubstantiated scientific claims or preliminary data.

Preprint Title Design, synthesis and investigation of water-soluble hemi-indigo photoswitches for bioapplications

Authors Daria V. Berdnikova

Publication Date 02 Sep 2019

Article Type Full Research Paper

Supporting Information File 1 Supporting Information.pdf; 1.5 MB

ORCID® iDs Daria V. Berdnikova - <https://orcid.org/0000-0002-0787-5753>

Design, synthesis and investigation of water-soluble hemi-indigo photoswitches for bioapplications

Daria V. Berdnikova*¹

Address: ¹ Department Chemie–Biologie, Organische Chemie II, Universität Siegen,
Adolf-Reichwein-Str. 2, 57076 Siegen, Germany

Email: berdnikova@chemie-bio.uni-siegen.de

* Corresponding author

Abstract

A series of hemi-indigo derivatives was synthesized and their photoswitching properties in aqueous medium were studied. The dimethoxy hemi-indigo derivative with the best photochromic performance in water was identified as a promising platform for the development of photoswitchable binders for biomolecules. The synthetic approach towards the introduction of the alkylamino pendant to the dimethoxy hemi-indigo core was developed that allowed to obtain an RNA-binding hemi-indigo derivative with photoswitchable fluorescent properties.

Keywords

hemi-indigo; photochromism; photoswitching; visible light; water solubility

Introduction

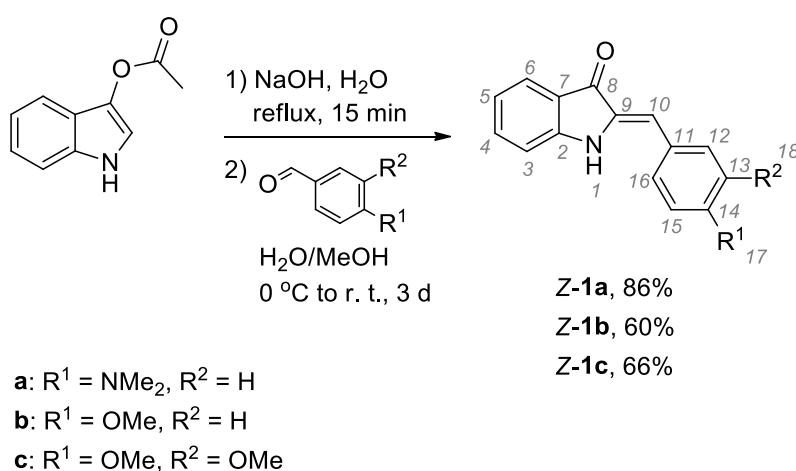
The application of organic photochromes in biological systems is fraught with their poor solubility and reduced photoswitching efficiency in aqueous medium. In many cases, approaches to improve the water solubility by chemical modification of photochromic scaffolds are not straightforward because the introduction of substituents often interferes with the desired photochemical properties. Along these lines, special efforts have been devoted to design, for example, water-soluble derivatives of spiropyran [1-3], azobenzene [4,5], diarylethene [6-8], or chromene [9] that keep efficient photochromism in aqueous medium. Although a significant progress has been made in the development of water-soluble photochromes, there is still an emerging search for new types of photochromic compounds for applications in biological systems. In particular, nowadays the development of photopharmacology is based mainly on azobenzene chemistry [10,11] and, therefore, finding of new biocompatible photochromes with complementary properties is highly desirable to speed up the progress in this important field. In this context, an emerging class of hemi-indigo photoswitches attracts special attention [12-16]. Despite the fact that the hemi-indigo dyes are known for more than 100 years [17], their photochemical properties are still essentially unexplored and no targeted studies on their photoswitching in aqueous media were performed. The hemi-indigo scaffold exists in two forms that can be photoswitched reversibly. The *Z*-isomer of hemi-indigo is thermodynamically stable whereas the *E*-isomer is metastable. The absorption spectrum of the *E*-isomer is bathochromically shifted relative to the one of the *Z*-isomer. Depending on the substitution pattern, the lifetime of metastable *E*-isomers varies from hours to days and sometimes even years [12-14]. Unlike most of the widely applied photochromes (spiropyranes, spirooxazines, chromenes, dithienylethenes etc.), both forms of hemi-

indigo absorb in the visible light range. Therefore, photochemical switching does not require the use of the UV light, which is of high importance for biological applications. Herein, the synthesis and adjustment of the substitution pattern of hemi-indigo derivatives for the efficient photoswitching in aqueous medium are described. Detailed characterization of the photoinduced isomerization of hemi-indigo derivatives in water is provided. Additionally, synthetic peculiarities of the introduction of an RNA-affine alkylamino substituent to the hemi-indigo scaffold are discussed.

Results and Discussion

Synthesis of Hemi-Indigo Derivatives Z-1a–1c

Synthesis of hemi-indigo derivatives **Z-1a–1c** with different substitution pattern of the phenyl ring was performed using the aldol condensation of indoxyl-3-acetate with corresponding benzaldehydes under alkaline conditions (Scheme 1) [13]. All compounds **1a–1c** were obtained in good yields as pure *Z*-isomers as supported by the NMR data (Figures S5–S13, Supporting Information).

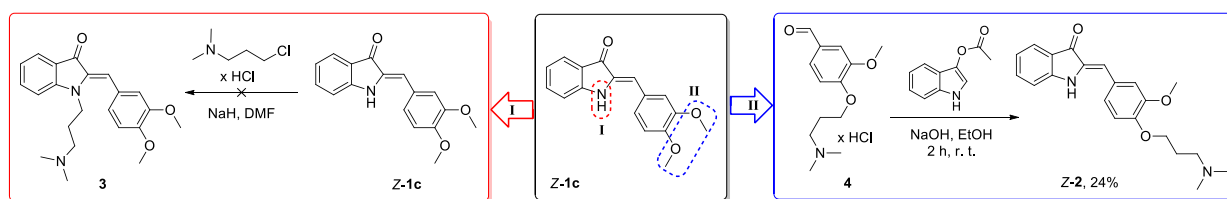


Scheme 1: Synthesis of hemi-indigo derivatives **Z-1a–1c**.

Introduction of an Alkylamino Substituent to the Hemi-Indigo Scaffold

Scaffold

Based on the data on photoswitching in water (*vide supra*), the dimethoxy-substituted hemi-indigo **Z-1c** was selected as a core structure for the design of RNA binders with photoswitchable properties [12]. To increase the solubility in aqueous medium and potential RNA-binding properties, the dimethylaminopropyl substituent [18] was introduced to hemi-indigo **Z-1c**. Two synthetically straightforward approaches of the alkylamino group introduction were considered: (i) *N*-alkylation of the indoxyl core and (ii) *O*-alkylation of the dimethoxyphenyl residue (Scheme 2).



Scheme 2: Synthetic routes to alkylamino-substituted dimethoxy hemi-indigo **Z-1c**.

Surprisingly, compound **3** (Method I) could not be obtained due to the cleavage of the C=C double bond in the course of the reaction followed by extensive destruction of the heterocyclic fragment. Variation of the reaction conditions, e.g. reduction of the reaction temperature and time, changing the ratio of the reactants and addition of NaI as a catalyst, did not suppress this decomposition to significant extent. A possible reason for this side process is the reactivity of the double bond carbon atom (Michael acceptor) [19]. The intramolecular nucleophilic attack of the introduced alkylamino group can possibly lead to the immediate double bond cleavage in **3**. This results in formation of unstable indoxyl that undergoes further destruction and veratraldehyde that is detected in the reaction mixture by NMR. This assumption is supported by the

observation that only one hemi-indigo derivative bearing an alkylamino substituent on the indoxyl N atom has been reported, so far [19]. The double-bond H atom in the latter compound is substituted with a cyano group that prevents nucleophilic cleavage by the alkylamino group.

Modification of the phenyl ring by Method II was successful and allowed to obtain the desired hemi-indigo **2** as a pure *Z*-isomer with 24% yield (Scheme 2) [12]. Importantly, the synthesis of *Z*-**2** required milder conditions and shorter reaction times than that of derivatives *Z*-**1a–1c**. Thus, the use of the water–methanol mixture as a solvent, heating and extended reaction times of more than 2 h resulted in the destruction of the desired product *Z*-**2**. At the same time, performance of the reaction at room temperature in pure ethanol allowed to increase the yield of *Z*-**2** and reduce the number of side-products. Purification of hemi-indigo *Z*-**2** by conventional column chromatography was not efficient. Pure product *Z*-**2** was obtained by gel filtration chromatography on sephadex (MeOH). The isolated compound *Z*-**2** is stable in a free base form whereas as a hydrochloride salt it slowly decomposes.

Optical Properties and Photoswitching in Aqueous Medium

Hemi-indigo derivatives *Z*-**1a–1c** display intense long-wavelength absorption bands, whose maxima are clearly dependent on the strength of the electron-donating substituent in the 4-position of the phenyl ring (Figure 1, Table 1). Thus, exchange of the 4-amino group in *Z*-**1a** to the 4-methoxy group in *Z*-**1b** resulted in the significant blue shift of the absorption maximum ($\Delta\lambda = 42$ nm). Notably, introduction of the second methoxy group to the 3-position of the phenyl ring in *Z*-**1c** did not shift the absorption maximum and just slightly affected the extinction (Table 1). Hemi-indigo derivatives *Z*-**1a–1c** are not fluorescent in aqueous solution.

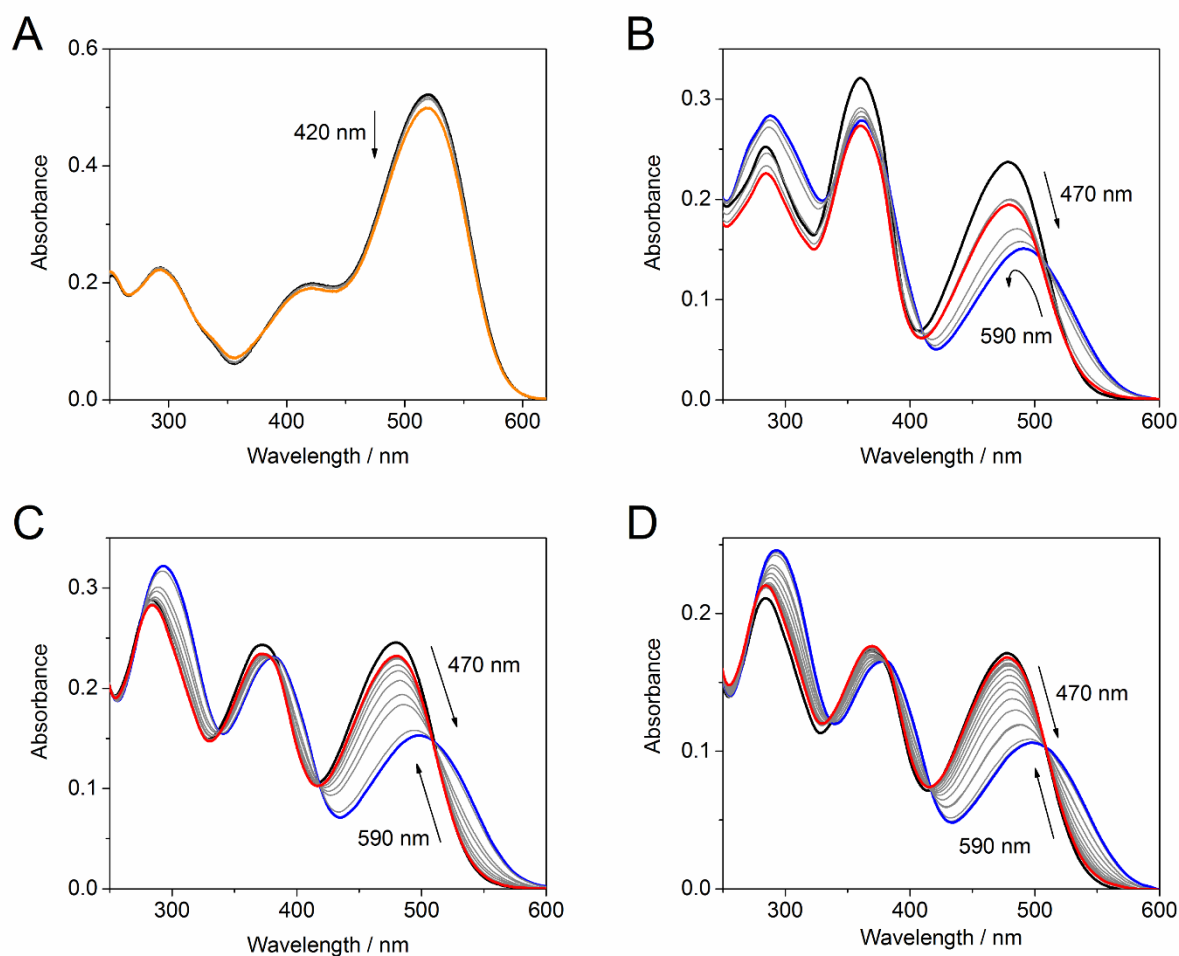


Figure 1: Photoswitching of hemi-indigo derivatives: (A) **Z-1a**, $c = 20 \mu\text{M}$ in H_2O with 10% (v/v) DMSO, $\lambda_{\text{ex}} = 420 \text{ nm}$; (B) **Z-1b**, $c = 20 \mu\text{M}$ in H_2O with 2% (v/v) EtOH, $\lambda_{\text{ex}} = 470 \text{ nm}$ (forward reaction) and 590 nm (backward reaction); (C) **Z-1c**, $c = 20 \mu\text{M}$ in H_2O with 2% (v/v) EtOH, $\lambda_{\text{ex}} = 470 \text{ nm}$ (forward reaction) and 590 nm (backward reaction); (D) **Z-2**, $c = 15 \mu\text{M}$ in H_2O , $\lambda_{\text{ex}} = 470 \text{ nm}$ (forward reaction) and 590 nm (backward reaction), $20 \text{ }^\circ\text{C}$. Spectra of the initial *Z*-isomers: black; PSS⁴²⁰: orange; PSS⁴⁷⁰: blue; PSS⁵⁹⁰: red.

Surprisingly, almost no switching of the dimethylamino-substituted hemi-indigo **Z-1a** was observed in water with 10% DMSO, i.e. only irradiation with violet light (420 nm) led to the residual isomerization (Figure 1A). Additionally, the hemi-indigo **Z-1a** was hardly soluble in aqueous medium and rather fast precipitation took place even in the presence of the co-solvent. Comparison with the reported data on **Z-1a** [13] and related hemi-indigo derivatives containing a 4-amino group in the phenyl ring [13] allowed to conclude that this substitution pattern is unfavorable for photoswitching in aqueous medium. Thus, a higher content of organic co-solvents (20-30% of DMSO, DMF or THF) or/and the presence of triethylamine was required to stimulate the photoswitching of the reported compounds with a 4-amino group in the phenyl ring [13]. Considering the limitations imposed on the nature and content of organic co-solvents used in biological studies, the dimethylamino derivative **Z-1a** was excluded from further studies.

In contrast, mono- and dimethoxy-substituted hemi-indigo derivatives **Z-1b** and **Z-1c** showed pronounced spectral changes upon irradiation indicating efficient *Z-E* isomerization of the C=C double bond (Figures 1B and 1C). The most complete *Z-E* conversion for both compounds **Z-1b** and **Z-1c** was achieved upon irradiation with blue light (470 nm) (cf. Figures S1 and S2, Supporting Information). The photoreactions proceeded rather fast and the photostationary state PSS⁴⁷⁰ was reached in 2.5 min for compound **Z-1b** and in 3.0 min for compound **Z-1c**. The backward *E-Z* conversion from PSS⁴⁷⁰ was performed upon irradiation by 590 nm (amber) light and occurred much slower (Table 1). In the case of mono-methoxy derivative **E-1b**, the backward reaction from PSS⁴⁷⁰ proceeded successfully during ca. 2 h of irradiation; then the isosbestic point was lost and the absorption intensity started decreasing due to slow precipitation of the compound from the aqueous solution (Figure 1B). The presence of the second methoxy group ensured better stability of the aqueous solution of dimethoxy derivative

Z-1c. In this case, the backward *E-Z* isomerization of *E-1c* from PSS⁴⁷⁰ took place within 5 h resulting in almost complete restoration of the initial absorbance of *Z-1c* in the PSS⁵⁹⁰ (Figure 1C). Investigation of the photostationary mixtures by fluorescence spectroscopy revealed that the photoinduced isomers *E-1b* and *E-1c* are not fluorescent in aqueous medium. Analysis of the isomeric compositions of the photostationary states was performed by Fischer method [20] because NMR-spectroscopic analysis was precluded by insufficient solubility or/and possible aggregation at higher concentrations. Thus, the Fischer method allowed to calculate the absorption spectra of pure *E*-isomers of **1b** and **1c** in water (Figure 2) as well as to evaluate the extent of the *Z-E* conversion in PSS⁴⁷⁰ and PSS⁵⁹⁰ (Table 1).

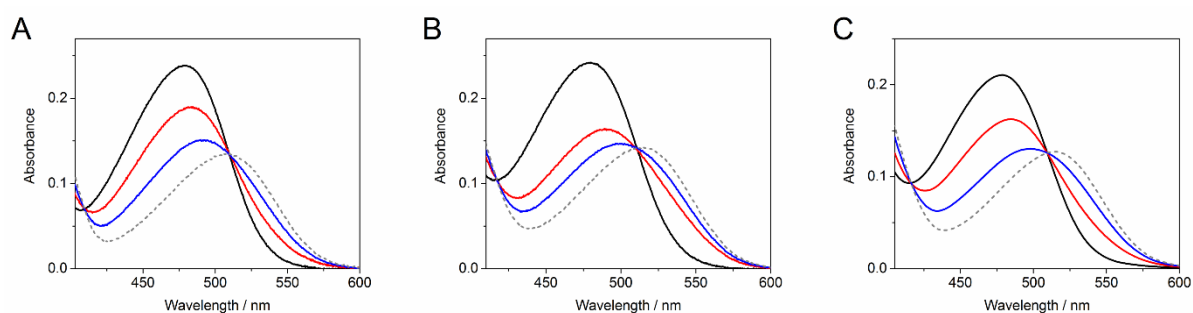


Figure 2: Absorption spectra of the *Z*-isomer (black), two photostationary states obtained upon irradiation with 520 nm (red) and 470 nm (blue) light for (A) **1b**, (B) **1c**, (C) **2** in water, $c = 20 \mu\text{M}$, $20 \text{ }^\circ\text{C}$. Grey dashed line represents the spectra of the corresponding *E*-isomers calculated by Fischer method.

The dimethoxy-derivative *Z-1c* showed better *Z-E* conversion in PSS⁴⁷⁰ and larger difference between the absorption maxima of the *Z*- and *E*-forms. At the same time, introduction of the second methoxy group to the phenyl ring resulted in the decrease of the *Z-E* isomerization quantum yield and reduced the half-life of *E-1c* in comparison to *E-1b* (Table 1). Nevertheless, the dimethoxy-substituted hemi-indigo *Z-1c* was

selected as a core structure for the design of photoswitchable RNA-binders due to higher conversion and better solubility in water.

Introduction of the alkylamino pendant provided compound **Z-2** with much better solubility in water. At the same time, the presence of the alkylamino group only slightly influenced the photochemical and photophysical characteristics of hemi-indigo **Z-2** in comparison with the parent compound **Z-1c** (Figure 1D, Figure 2C, Table 1). Thus, the positions of the absorption maxima of both *Z*- and *E*-forms, the extents of conversion in PSS, the photoisomerization quantum yields as well as the half-lives of the photoinduced forms appeared to be almost independent of the presence of the alkylamino substituent. Interestingly, comparison with the data obtained for hemi-indigo **Z-2** in aqueous 10 mM Na-phosphate buffer containing 0.1 M NaCl, pH = 7.0 [12], showed that the increase in the ionic strength of the medium resulted in drastic decrease of the half-life of the photoinduced form *E-2* whereas other characteristics remained almost unaffected (Table 1). This indicates that highly ionic medium reduces the energy barrier in the ground state responsible for the rate of thermal *E-Z* isomerization pointing out the importance of the coulomb interactions between hemi-indigo and buffer components. Comparison with structurally related hemi(thio)indigo dyes allows to assume that the energy maximum in the ground state of hemi-indigo corresponds to the 90° rotation about the central double bond resulting in formation of the state with biradical-like character that is polarized along the molecule's long axis [21]. Highly polar medium stabilizes this state leading to the decrease of the energy barrier between *Z*- and *E*-isomers and, therefore, reducing the half-life of the *E*-form. Recently, a proof-of-principle for the application of hemi-indigo derivative **Z-2** as a binder for the human immunodeficiency virus type 1 (HIV-1) RNA with photoswitchable fluorescent properties was provided [12]. It was shown that hemi-indigo **Z-2** associates with the regulatory elements of HIV-1 genome RNA with high affinity ($K_b \sim 10^5 \text{ M}^{-1}$)

while keeping its photoswitching properties. Both initial *Z-2* and photoinduced *E-2* forms of hemi-indigo remain bound to RNA. Most notably, the interaction of *Z-2* with HIV-1 RNA produces a remarkable light-up effect whose extent depends on the particular sequence of RNA. Photoswitching of the RNA-bound hemi-indigo *Z-2* to the *E*-form results in emission quenching. The ON–OFF fluorescence switching of *Z-2*–RNA complexes can be performed reversibly by repeated irradiation with blue (470 nm) and amber (590 nm) light.

Conclusions

To sum up, hemi-indigo derivatives with different substitution pattern in the phenyl ring were synthesized and their photochemical behaviour in aqueous medium was studied. The presence of a methoxy group at the 4-position of the phenyl ring was identified as a necessary condition for the efficient photoswitching of hemi-indigo in water. At the same time, the presence of a strong electron-donating dimethylamino group at this position is unfavorable for the photoswitching in water. It was also shown that the introduction of the second methyl group to the 3-position of the phenyl ring improves the water solubility of the photoswitch and increases the red shift of the absorption maximum of the *E*-isomer. As a further step, the synthetic approach towards the attachment of the RNA-affine alkylamino substituent was developed. Overall, the hemi-indigo derivatives were introduced as promising photoswitches for aqueous media possessing valuable properties for bioapplications.

Experimental

Materials and Equipment

Reagents and solvents were obtained from commercial sources (Acros, Merck, Fischer) and used as received. Reactions were monitored on POLYGRAM[®] SIL G/UV₂₅₄ (Macherey-Nagel) TLC plates with detection by UV light irradiation (254 nm or 366 nm). Column chromatography was performed on Sephadex[®] columns.

¹H NMR and ¹³C NMR spectra were recorded on a *JEOL ECZ 500* spectrometer at 25 °C using 5 mm tubes. Chemical shifts were determined with accuracy of 0.01 ppm and 0.1 ppm for ¹H and ¹³C spectra, respectively, and are given relative to the residual signal of the solvent that was used as internal standard (DMSO-*d*₆: $\delta_{\text{H}} = 2.50$ ppm, $\delta_{\text{C}} = 39.5$ ppm). Spin–spin coupling constants for the proton spectra were determined with accuracy of 0.2 Hz. The proton NMR signal assignments were performed using COSY and ROESY 2D NMR techniques. The carbon NMR signal assignments were performed by means of HSQC and HMBC 2D NMR techniques. Mass spectra (ESI) were recorded on a *Finnigan LCQ Deca* mass-spectrometer. Elemental analysis was performed with a *HEKAtech EUROEA* combustion analyser by Mr. Rochus Breuer (Universität Siegen, Organische Chemie I). Melting points were measured with a *BÜCHI 545* (BÜCHI, Flawil, CH) melting point apparatus in open capillaries and are uncorrected. Electronic absorption spectra were measured on a *Cary 100 Bio* two-beam spectrophotometer and a *Specord 600* (Analytik Jena AG) diode-array spectrophotometer. Fluorescence spectra were recorded on a *Cary Eclipse* spectrofluorimeter. Optical spectroscopy measurements were performed in thermostated quartz sample cells of 10 mm pathlength. Preparation and handling of the solutions were carried out under red light.

Photochemical reactions were performed using the following LED light sources: *LUMOS* (360 nm); *Roithner* H2A1-H420 130 mW (420 nm); *Roschwege* HighPower-LED Blau (470 nm); *Roschwege* HighPower-LED Grün (520 nm); *Roschwege* HighPower-LED Amber (590 nm).

Synthesis

Synthesis and characterization of hemi-indigo derivative **Z-2** are described in detail in Ref. 12.

General procedure for the synthesis of hemi-indigo derivatives **Z-1a–1c**

Under argon gas atmosphere, a solution of indoxyl-3-acetate (200 mg, 1.14 mmol) in aqueous NaOH (1.5 M, 6.2 mL, degassed) was heated at 100 °C for ca. 15 min. Then the mixture was cooled to 0 °C and the solution of the corresponding benzaldehyde in 1–2 mL MeOH (Ar-degassed) was added upon vigorous stirring [for compound **Z-1a**: 4-(dimethylamino)benzaldehyde (170 mg, 1.14 mmol); for compound **Z-1b**: *p*-anisaldehyde (155 mg, 1.14 mmol); for compound **Z-1c**: veratraldehyde (189 mg, 1.14 mmol)]. After addition of the aldehyde, the mixture was warmed up to the ambient temperature and stirred for 3 days. Then the mixture was neutralized with 1M aq. HCl and extracted with EtOAc. The combined organic layers were dried with Na₂SO₄ and the solvent was removed by distillation. The obtained solid was redissolved in EtOH and filtered to remove the insoluble precipitate of indigo side-product. After filtration, the solvent was partially removed and the pure *Z*-isomer of the corresponding product was crystallized at –20 °C.

(Z)-2-(4-(dimethylamino)benzylidene)indolin-3-one (**Z-1a**)

Deep violet needles, yield 86% (259 mg, 0.98 mmol), mp 232–234 °C (Lit.: 235–236 °C) [13], R_f = 0.67 (hexane/EtOAc 1:1 v/v). ^1H NMR (500 MHz, DMSO- d_6 , δ ppm, J Hz): 3.00 (s, 6H, H-17); 6.64 (s, 1H, H-10), 6.78 (d, 2H, H-13, H-15, J = 9.0); 6.88 (ddd, 1H, H-4, J = 7.8, 7.0, 0.7); 7.14 (d, 1H, H-3, J = 8.1); 7.47 (ddd, 1H, H-5, J = 8.3, 7.1, 1.3); 7.55 (d, 1H, H-6, J = 8.3); 7.61 (d, 2H, H-12, H-16, J = 8.8), 9.55 (s, 1H, H-1). ^{13}C NMR (126 MHz, DMSO- d_6 , δ ppm): 39.7 (2C, C-17); 112.1 (2C, C-13, C-15); 112.5 (1C, C-3); 112.6 (1C, C-10); 119.1 (1C, C-4); 120.5 (1C, C-7); 121.3 (1C, C-11); 123.7 (1C, C-6); 131.72 (2C, C-12, C-16); 131.68 (1C, C-9); 135.3 (1C, C-5); 150.3 (1C, C-14); 153.3 (1C, C-2); 185.2 (1C, C-8). El. Anal. calcd. (%) for $\text{C}_{17}\text{H}_{16}\text{N}_2\text{O}$: C, 77.25; H, 6.10; N, 10.60; found: C, 77.05; H, 6.13; N, 10.39. ESI-MS **Z-1a** in MeOH, m/z : 263 [**Z-1a-H**] $^-$, 264 [**Z-1a**] $^+$, 265 [**Z-1a+H**] $^+$.

(Z)-2-(4-methoxybenzylidene)indolin-3-one (**Z-1b**)

Brownish-golden powder, yield 60% (172 mg, 0.68 mmol), mp 180–181 °C (Lit.: 180–181 °C) [20], R_f = 0.75 (hexane/EtOAc 1:1 v/v). ^1H NMR (500 MHz, DMSO- d_6 , δ ppm, J Hz): 3.82 (s, 3H, H-17); 6.65 (s, 1H, H-10); 6.90 (t, 1H, H-4, J = 7.8); 7.04 (d, 2H, H-13, H-15, J = 8.8); 7.14 (d, 1H, H-3, J = 8.1); 7.51 (ddd, 1H, H-5, J = 8.4, 7.1, 1.1); 7.57 (d, 1H, H-6, J = 7.6); 7.71 (d, 2H, H-12, H-16, J = 8.8); 9.68 (s, 1H, H-1). ^{13}C NMR (126 MHz, DMSO- d_6 , δ ppm): 55.3 (1C, C-17); 110.5 (1C, C-10); 112.6 (1C, C-3); 114.6 (2C, C-13, C-15); 119.5 (1C, C-4); 120.2 (1C, C-7); 123.9 (1C, C-6); 126.6 (1C, C-11); 131.7 (2C, C-12, C-16); 133.1 (1C, C-9); 136.0 (1C, C-5); 153.9 (1C, C-2); 159.6 (1C, C-14); 186.0 (1C, C-8). El. Anal. calcd. (%) for $\text{C}_{16}\text{H}_{13}\text{NO}_2$: C, 76.48; H, 5.21; N, 5.57; found: C, 76.31; H, 5.15; N, 5.50. ESI-MS **Z-1b** in MeOH, m/z : 250 [**Z-1b-H**] $^-$.

(Z)-2-(3,4-dimethoxybenzylidene)indolin-3-one (**Z-1c**)

Orange crystals, yield 66% (211 mg, 0.75 mmol), mp 191–192 °C, R_f = 0.56 (hexane/EtOAc 1:1 v/v). ^1H NMR (500 MHz, DMSO- d_6 , δ ppm, J Hz): 3.82 (s, 3H, H-18); 3.85 (s, 3H, H-17); 6.66 (s, 1H, H-10); 6.91 (t, 1H, H-4, J = 7.8); 7.06 (d, 1H, H-15, J = 8.4); 7.14 (d, 1H, H-3, J = 8.1); 7.29 (d, 1H, H-12, J = 2.0); 7.35 (dd, 1H, H-16, J = 8.7, 2.0); 7.51 (ddd, 1H, H-5, J = 8.3, 6.9, 1.1); 7.58 (d, 1H, H-6, J = 7.6); 9.66 (s, 1H, H-1). ^{13}C NMR (126 MHz, DMSO- d_6 , δ ppm): 55.6 (1C, C-18); 55.7 (1C, C-17); 111.1 (1C, C-10); 112.0 (1C, C-15); 112.7 (1C, C-3); 113.8 (1C, C-12); 119.6 (1C, C-4); 120.4 (1C, C-7); 123.3 (1C, C-16); 123.9 (1C, C-6); 126.8 (1C, C-11); 133.3 (1C, C-9); 136.0 (1C, C-5); 148.9 (1C, C-14); 149.5 (1C, C-13); 154.0 (1C, C-2); 186.0 (1C, C-8). El. Anal. calcd. (%) for $\text{C}_{17}\text{H}_{15}\text{NO}_3$: C, 72.58; H, 5.37; N, 4.98; found C, 72.80; H, 5.27; N, 4.89. ESI-MS **Z-1c** in MeOH, m/z : 280 [**Z-1c-H**] $^-$.

Supporting Information

Supporting Information File 1: Additional spectral data, detailed description of the experiments performed, ^1H NMR of compounds **Z-1a–1c** and LED characteristics.

File Format: pdf

Acknowledgements

This project has received funding from the European Union's Horizon 2020 research and innovation programme, Marie Skłodowska-Curie actions (MSCA), under grant agreement No 749788 – PHOTORNA. I thank Prof. Dr. Heiko Ihmels (Universität Siegen, Germany) for fruitful discussions and valuable advices.

References

1. Özçoban, C.; Halbritter, T.; Steinwand, S.; Herzig, L.-M.; Kohl-Landgraf, J.; Askari, N.; Groher, F.; Fürtig, B.; Richter, C.; Schwalbe, H.; Suess, B.; Wachtveitl, J.; Heckel, A. *Org. Lett.*, **2015**, *17*, 1517–1520.
2. Kohl-Landgraf, J.; Braun, M.; Özçoban, C.; Gonçalves, D. P. N.; Heckel, A.; Wachtveitl, J. *J. Am. Chem. Soc.*, **2012**, *134*, 14070–14077.
3. Kaiser, C.; Halbritter, T.; Heckel, A.; Wachtveitl, J. *Chem. Select*, **2017**, *2*, 4111–4123.
4. Bergen, A.; Rudiuk, S.; Morel, M.; Le Saux, T.; Ihmels, H.; Baigl, D. *Nano Lett.*, **2016**, *16*, 773–780.
5. Zhang, Z.; Burns, D. C.; Kumita, J. R.; Smart, O. S.; Woolley, G. A. *Bioconjugate Chem.*, **2003**, *14*, 824–829.
6. Tong, Z.; Pu, S.; Xiao, Q.; Liu, G.; Cui, S. *Tetrahedron Lett.*, **2013**, *54*, 474–477.
7. Pu, S.; Liu, H.; Liu, G.; Chen, B.; Tong, Z. *Tetrahedron*, **2014**, *70*, 852–858.
8. Zou, Y.; Yi, T.; Xiao, S.; Li, F.; Li, C.; Gao, X.; Wu, J.; Yu, M.; Huang, C. *J. Am. Chem. Soc.*, **2008**, *130*, 15750–15751.
9. Paramonov, S. V.; Lokshin, V.; Ihmels, H.; Fedorova, O. A. *Photochem. Photobiol. Sci.*, **2011**, *10*, 1279–1282.
10. Velema, W. A.; Szymanski, W.; Feringa, B. L. *J. Am. Chem. Soc.*, **2014**, *136*, 2178–2191.
11. Hüll, K.; Morstein, J.; Trauner, D. *Chem. Rev.*, **2018**, *118*, 10710–10747.
12. Berdnikova, D. V. *Chem. Commun.*, **2019**, *55*, 8402–8405.
13. Petermayer, C.; Thumser, S.; Kink, F.; Mayer, P.; Dube, H. *J. Am. Chem. Soc.*, **2017**, *139*, 15060–15067.
14. Petermayer, C.; Dube, H. *J. Am. Chem. Soc.*, **2018**, *140*, 13558–13561.

15. Ikegami, M.; Arai, T. *Bull. Chem. Soc. Jpn.*, **2003**, *76*, 1783–1792.
16. Ikegami, M.; Arai, T. *Chem. Lett.*, **2005**, *34*, 492–493.
17. Baeyer, A. *Ber. Dtsch. Chem. Ges.*, **1883**, *16*, 2188–2204.
18. Thomas, J. R.; Hergenrother, P. J. *Chem. Rev.*, **2008**, *108*, 1171–1224.
19. Velezheva, V. S.; Brennan, P. J.; Marshakov, V. Yu.; Gusev, D. V.; Lisichkina, I. N.; Peregudov, A. S.; Tchernousova, L. N.; Smirnova, T. G.; Andreevskaya, S. N.; Medvedev, A. E. *J. Med. Chem.*, **2004**, *47*, 3455–3461.
20. Fischer, E. *J. Phys. Chem.*, **1967**, *71*, 3704–3706.
21. Wiedbrauk, S.; Dube, H. *Tetrahedron Lett.*, **2015**, *56*, 4266–4274.